

Semi-microscopic construction of multi- α cluster spaces

J. R. M. Berriel-Aguayo¹ and P. O. Hess^{1,2}

¹ *Instituto de Ciencias Nucleares, Universidad Nacional Autónoma de México, Circuito Exterior, C.U., A.P. 70-543, 04510 México D.F., Mexico*

² *Frankfurt Institute for Advanced Studies, Johann Wolfgang Goethe Universität, Ruth-Moufang-Str. 1, 60438 Frankfurt am Main, Germany*

May 30, 2022

Abstract

An approximate but straight forward projection method to molecular many α -particle states is proposed and the overlap to the shell model space is determined. The resulting space is in accordance with the shell model, but still contains states which are not completely symmetric under permutations of the α -particles, which is one reason to call the construction *semi-microscopic*. A new contribution is the construction of the 6- and 7- α -particle spaces. The errors of the method propagate toward larger number of α -particles and larger shell excitations. In order to show the effectiveness of the construction proposed, the so obtained spaces are applied, within an algebraic cluster model, to ^{20}Ne , ^{24}Mg and ^{28}Si , each treated as a many- α -particle system. Former results on ^{12}C and ^{16}O are resumed

1 Introduction

Cluster physics has always enjoyed a great interest, because it enlightens the structure of nuclei and provides a manageable method to treat, in general, many cluster systems, avoiding the very large shell model space. [1]. In particular, the α -cluster structure plays an important role in understanding the microscopic underpinning of light

and heavy nuclei. For a recent review on the experimental findings and theoretical ones on the cluster structure in light nuclei, see [2] and [3], respectively.

An essential ingredient of any cluster model is the construction of the Hilbert space. For example, in [4] a microscopic projection method was applied for the construction of up to the 5- α particle space, besides other exotic cluster configurations. The method is quite involved and requires to calculate integral kernels, which are, however, subject to numerical errors.

The α -cluster structure is important in several areas, as decay modes of light and heavy nuclei (for example in the reaction $\alpha + {}^{16}\text{O}$), fusion reactions in heavy stars and investigations of α -particle condensates in nuclei [5]. This illustrates the necessity to obtain the Hilbert space for any number of α -particle systems, without recurring to involved methods for the construction of these spaces.

The main objective of this contribution is to introduce an iterative procedure to obtain, at least approximately, the microscopic space for any number of α -particle system, which at the same time is practical and straight forward to apply. The method is based only on algebraic manipulations and we intend to convince that an approximate projection is favored over an exact one. We will see that for systems of few α -particles it works for low lying states and it does not suffer from involved manipulations as in [4]. Especially, we will see that the results in [4] also suffer from states which are not part of the shell model space and that the origin lies in the calculation of overlap matrix elements which generates numerical errors. However, the price to pay for the approximation we use, is the inclusion of states which are not completely symmetric in the permutations of the α -particles.

The α -cluster spaces are by itself useful for any theory on many α -cluster systems. In order to illustrate the application of the classification we will only apply a phenomenological and algebraic cluster model, namely the so-called *Semimicroscopic Algebraic Cluster Model* (SACM) [6, 7], which in most cases is effective in two-cluster systems, also as an alternative to the geometric description of a two-cluster system [8, 9]. Spectra, transition values and spectroscopic factors are also calculated.

In what follows, the iterative procedure will be explained, which is applied to 3 (${}^{12}\text{C}$), 4 (${}^{16}\text{O}$), 5 (${}^{20}\text{Ne}$), 6 (${}^{24}\text{Mg}$) and and 7 (${}^{28}\text{Si}$) α -particle states. A new contribution is the list of 6- and 7- α particle states.

The paper is structured as follows: In Section 2 the iterative procedure is explained, whose results will be compared to [4] for up to 5 α -particles, where we will also prove that the space of the 5- α system, as determined in [4], includes states which are not allowed by the PEP. In Section 3 we apply the results obtained to systems of up to 7 α -particles. In Section 4 Conclusions will be drawn. In the Appendix we construct explicitly the 5 α -particle space of $0\hbar\omega$ and $1\hbar\omega$.

2 Approximate construction of the multi α -particle space

The objective is to construct a basis for a multi α cluster systems, whose states are classified by a ket, depending on $SU(3)$ quantum numbers, the natural choice for the shell model. The molecular basis has an overlap to the shell model, which is easy to satisfy. The main difficulty is to achieve that these basis states also are symmetric under the interchange of any two α particles. The method is approximate, with the goal that at least states which are low lying in energy are symmetric under the permutation of the α particles. The result will be compared to existing constructions of 3-, 4- and 5- α particle systems.

The construction of the multi- α particle space is divided into two steps:

- **Step 1:** Construction of molecular α -particle states. The α -particles will be added successively in such a manner that the symmetry between them is at least approximately satisfied.
- **Step 2:** The shell model space is explicitly constructed, to which the molecular states are compared and the overlap is determined. The resulting states are the ones which are taken into account as part of the model space. With increasing $n\hbar\omega$ shell excitations, more and more states arise, which are not symmetric under the interchange of α -particles and also the multiplicity is larger than for the allowed ones. Fortunately, for low n -values and/or large eigenvalues of the second order $SU(3)$ Casimir operator, the space is free of these spurious states.

Before proceeding, we have to spend some words on the definition of clusterization, there are two definitions: The weak and the strong one. In the strong definition, the nuclear subsystem has to exhibit an

explicit spatial separation from the other clusters, while in the weak definition this is not the case, only requiring that the cluster state has an overlap to the state of the united nucleus. E.g., for a two-cluster system the overlap is $\langle \Psi | \psi_{c_1} \psi_{c_2} R \rangle$, where $|\Psi\rangle$ is the state of the united nucleus, ψ_{C_k} ($k = 1, 2$) are the cluster states and R is the relative wave function. For example, the ground state of ^{16}O is a spherical nucleus which has an overlap to the cluster state of $^{12}\text{C} + \alpha$, thus it shows a clusterization in the weak sense but not in the strong sense, because ^{26}O is spherical. Here, we apply the definition of the weak clusterization.

2.1 Iterative procedure for the molecular states

In the construction of the molecular states we proceed as follows: The relative position of n α -particles are traced via $(n - 1)$ *Jacobi-coordinates*, where $\vec{\lambda}_k$ ($k = 1, 2, \dots, n - 1$) is the Jacobi coordinate between the $(k + 1)$ 'st α -particle and the center of mass of the subsystem of the first k α -particles.

Each of these $\vec{\lambda}_k$ refer to a relative motions, which is described by an harmonic oscillator, and therefore carry N_{λ_k} oscillation quanta.

We impose the restriction

$$N_{\lambda_1} \geq N_{\lambda_2} \geq \dots \geq N_{\lambda_{n-1}} \quad . \quad (1)$$

With the restriction (1) the original state and the one where the N_{k_1} is interchanged with N_{k_2} are treated as equal, corresponding to having permuted the two α particles. Thus, the two states are symmetric to each other: Under the permutation of the particle k_1 with k_2 , the states change accordingly

$$P_{k_1, k_2} | N_1 \dots N_{k_1} \dots N_{k_2} \dots N_{k_{n-1}} \rangle = | N_1 \dots N_{k_2} \dots N_{k_1} \dots N_{k_{n-1}} \rangle \quad . \quad (2)$$

The $SU(3)$ -irreducible representations (irreps) are obtained by multiplying successively the $SU(3)$ irreps of the k - α -particle space with $(N_{\lambda_{k+1}}, 0)$, imposing the condition (1). In this manner, the state (2) describes approximately a symmetric α -particle configurations. An explicit symmetrization, as done in [4] or in [10, 11], is not applied. We also do not construct the coordinate representation of the cluster wave function, but rather use the ket-notation. The advantage is that

we only need to demand that the quantum numbers correspond to a state of a multi- α particle configuration, with an overlap to a state within the shell model with the same quantum numbers. The disadvantage, though, is that we cannot address the strong definition of clusterization.

In this manner, we obtain iteratively the space of 3- to 7- α -particle states, listed in the Tables 1, 2, 3, 4 and 5. The procedure does not involve an *explicit* construction of symmetric states, but only partially by the above condition imposed. The result is compared to the shell model space, whose construction is explained in the Appendix at hand of the $1\hbar\omega$ excitation of ^{20}Ne .

The advantage of the method proposed is the direct extension to any number of α -particles.

The obtained approximate n α -particle space are compared to the work of Horiuchi [12] and Katō [4]. For small $\hbar\omega$ excitations the list is *identical* and for large $\hbar\omega$ excitations, some differences in the multiplicity of *high lying states* (smaller eigenvalue of the second order Casimir operator) appear and also some new irreps (i.e. not satisfying the symmetry property under permutations of the α -particles), but also with a smaller eigenvalue of the second order Casimir operator.

$n\hbar\omega$	(λ, μ)
0	(0,4)
1	(3,3)
2	(2,4), (4,3), (6,2)
3	(3,4), (5,3), (7,2), (9,1)
4	(4,4), (6,3), (8,2), (10,1), (12,0)
5	(5,4), (7,3), (13,0)
6	(6,4), (8,3), (10,2), (12,1)

Table 1: Model space of the ^{12}C nucleus within the SACM for up to $6\hbar\omega$ excitations. The content agrees with [12].

$n\hbar\omega$	Katō	present comilation
0	(0, 0)	(0, 0)
1	(2, 1)	(2, 1)
2	(2, 0) (3, 1) (0, 4) (4, 2)	(2, 0) ² (3, 1) (0, 4) (4, 2)
3	(3, 0) (0, 3) (2, 2) (4, 1) (3, 3) (6, 0) (5, 2) (2, 5) (6, 3)	<i>(0, 0)</i> <i>(1, 1)</i> ² (3, 0) ³ (0, 3) ² (2, 2) ² (4, 1) ³ <i>(1, 4)</i> (3, 3) (6, 0) (5, 2) (2, 5) (6, 3)

Table 2: Space of the 4- α -particle system. In italic we denote the irreps in the right column which do not appear in the left column. For $1\hbar\omega$ the (2, 0) irrep appears twice in the present calculation, while in [4] the multiplicity is one. At $3\hbar\omega$ excitation, besides an increase in the multiplicities also additional irreps appear in our compilation.

For the 3- α -particle case (Table 1) the list is identical to the one published by Horiuchi [12]. In Table 2 the space of the 4- α -particle system is compared to Katō's list. In Table 3, the same is done for the 5- α -particle system and in Tables 4 and 5 for the 6- and 7-particle case, respectively. While there is no difference in the 3- α particle space within the microscopic treatment and our approximation, the first difference appear in the 4- α -particle case, from $2\hbar\omega$ on. There, the irrep (2, 0) has a multiplicity of 2, while in [4] its is just one. As seen for $3\hbar\omega$ the multiplicity in our approach is raising significantly and also some additional irreps appear. This increase of the multiplicity indicates that many more states can be constructed, with the quantum numbers of an allowed shell model state but not with the right symmetry of the α -particles. However, these differences appear only for irreps with a lower eigenvalue of the second Casimir operator and, thus, are of lesser importance. One viable solution is to restrict to just multiplicity one, i.e., *implementing a further practical constraint*, with the price to pay that this eliminates additional states which are symmetric under permutations. With this, the problem of a too large

multiplicity is avoided. Note, that in a microscopic projection method the multiplicity also increases with larger $n \hbar\omega$ excitations.

The 4-particle case is a good test for the quality of the approximation, because exact procedures were published in [10] and the book [11]. Unfortunately, this method is quite involved for the 4- α -particle system. In general, with the new method we get the same $SU(3)$ -irreps, but with a larger multiplicity with increasing $n \hbar\omega$.

For the 5- α -particle state the $0\hbar\omega$ list is identical with the table of Katō, but for the $1\hbar\omega$ the discrepancies mentioned appear also for large $SU(3)$ irreps. In order to convince the reader, in the Appendix we explicitly construct the 0 and $1\hbar\omega$ shell model space of ^{20}Ne and show that some states listed in [4] are indeed not part of the shell model space, suggesting possible difficulties of the numerical procedure applied in [4] in calculating the overlap matrix elements (kernels). Eliminating those states, a good agreement is reached again.

The present section also provides the new contribution of 6- and 7- α particle states up to large $n \hbar\omega$. The result is useful for any cluster model which relies on a microscopic Hilbert space, i.e., independent on what will be presented in the next section. The procedure proposed can be directly extended to a higher number of α -cluster states.

3 Applications

The usefulness of the deduced approximate Hilbert space of $n \alpha$ -particle systems is investigated in this section, at hand of the SACM. Results for ^{12}C and ^{16}O are resumed shortly, because these are already published in [13, 14]. Also, the space for ^{12}C is identical to the exact approach and for ^{16}O differences only appear from $2\hbar\omega$ excitations on and there only for small $SU(3)$ irreps, which do not have any sensible influence at low energy. Therefore, we restrict to systems with 5 (^{20}Ne), 6 (^{24}Mg) and 7 (^{28}Si) α -particles. In addition, instead of a full microscopic model, the more easy to apply SACM [6, 7] is chosen. The applicability was investigated many times, were we mention only one particular to a series of light nuclear two-cluster systems [15]. More than two clusters are mostly not considered, which makes this contribution also interesting from a conceptual point of view.

There are, however, restrictions to the SACM making it difficult to treat certain aspects of a cluster system. This is mainly related of not constructing a spatial representation of the system. Also the

states are stable and cannot decay in a dynamical way, thus, thresholds of cluster decays are difficult to simulate. Interesting situations, like the transition to an α -gas state, are very difficult to study. Nevertheless, spectra, transition rates and spectroscopic factors can still be obtained.

3.1 A particular SACM Hamiltonian, electromagnetic transition and spectroscopic factor operator

Here, not the most general Hamiltonian will be used but one which satisfies the needs for light nuclei [13, 14], namely

$$\begin{aligned}
\mathbf{H} = & \hbar\omega\mathbf{n}_\pi + \chi(1 - \chi_{n_\pi}\Delta\mathbf{n}_\pi)\mathbf{C}_2(\lambda, \mu) + t_3(\mathbf{C}_2(\lambda, \mu))^2 + t_1\mathbf{C}_3(\lambda, \mu) \\
& + (\xi + \xi_{Lnp}\Delta\mathbf{n}_\pi)\mathbf{L}^2 + t_2\mathbf{K}^2 \\
& + b_1 \left[(\boldsymbol{\sigma}^\dagger)^2 - (\boldsymbol{\pi}^\dagger \cdot \boldsymbol{\pi}^\dagger) \right] \cdot [h.c.] \quad .
\end{aligned} \tag{3}$$

The first term defines the scale of the harmonic oscillator shell, i.e., $\hbar\omega = 45 A^{-\frac{1}{3}} - 25 A^{-\frac{2}{3}}$ and it is fixed [16], A is the number of nucleons. The $\mathbf{C}_2(\lambda, \mu)$ is the second order Casimir operator of $SU(3)$, which is proportional to the quadrupole-quadrupole interaction [17]. The \mathbf{K}^2 term gives the square of the K -projection of the angular momentum onto the intrinsic z-axis and serves to distinguish states with the same angular momentum within a given $SU(3)$ irrep [18]. The b_1 -term is proportional to a Casimir operator of $SO(4)$ and mixes $SU(3)$ irreps. The \mathbf{L}^2 is the angular momentum operator with a factor simulating a variable moment of inertia. The remaining terms are corrections.

The $\tilde{\mathbf{C}}_2(\tilde{\lambda}, \tilde{\mu})$ is the second order Casimir-invariant of the coupled $\widetilde{SU}(3)$ group, having contributions both from the internal cluster part and from the relative motion. The $\tilde{\mathbf{C}}_2(\tilde{\lambda}, \tilde{\mu})$ is given by:

$$\begin{aligned}
\tilde{\mathbf{C}}_2(\tilde{\lambda}, \tilde{\mu}) &= 2\tilde{\mathbf{Q}}^2 + \frac{3}{4}\tilde{\mathbf{L}}^2, \\
&\rightarrow \left(\tilde{\lambda}^2 + \tilde{\lambda}\tilde{\mu} + \tilde{\mu}^2 + 3\tilde{\lambda} + 3\tilde{\mu} \right), \\
\tilde{\mathbf{Q}} &= \tilde{\mathbf{Q}}_C + \tilde{\mathbf{Q}}_R, \\
\tilde{\mathbf{L}} &= \tilde{\mathbf{L}}_C + \tilde{\mathbf{L}}_R,
\end{aligned} \tag{4}$$

where $\tilde{\mathbf{Q}}$ and $\tilde{\mathbf{L}}$ are the total quadrupole and angular momentum operators, respectively, and R refers to the relative motion. Thus, the second order Casimir operator describes the quadrupole-quadrupole interaction strength and determines the deformation of the nucleus. Within the $SU(3)$ -basis, the eigenvalue of $\tilde{\mathbf{C}}_2(\tilde{\lambda}, \tilde{\mu})$ is also indicated. The relations of the quadrupole and angular momentum operators to the $\tilde{C}_{2m}^{(1,1)}$ generators of the $\widetilde{SU}(3)$ group, expressed in terms of $\widetilde{SU}(3)$ -coupled π -boson creation and annihilation operators, are [19]:

$$\begin{aligned}\tilde{\mathbf{Q}}_{k,2m} &= \frac{1}{\sqrt{3}}\tilde{C}_{k2m}^{(1,1)}, \\ \tilde{\mathbf{L}}_{k1m} &= \tilde{C}_{k1m}^{(1,1)}, \\ \tilde{C}_{lm}^{(1,1)} &= \sqrt{2}\left[\pi^\dagger \otimes \pi\right]_{lm}^{(1,1)}.\end{aligned}\quad (5)$$

The term with the square of the second order Casimir operator serves to fine tune the relative positions of the band heads, which is also the case for the third order Casimir operator, whose eigenvalue within the $SU(3)$ -basis is given by

$$\tilde{\mathbf{C}}_3 \rightarrow (\lambda - \mu)(2\lambda + \mu + 2)(\lambda + 2\mu + 3) \quad , \quad (6)$$

These two correction terms improve slightly the adjustment of the band heads and are, therefore, of lesser importance.

The eigenvalue of the angular momentum operator is $L(L+1)$ and of \mathbf{K}^2 is just K^2 , where K is the projection of the angular momentum on the intrinsic z -axis.

The $\chi_{n\pi}$ term varies the quadrupole-quadrupole interaction with increasing shell excitations and the ξ_{Lnp} term does the same for the moment of inertia, which is inverse proportional to the factor of \mathbf{L}^2 .

The quadrupole electromagnetic transition operator is defined as

$$\mathbf{T}_m^{(E2)} = \sum_{\gamma} e_{\gamma}^{(2)} \mathbf{Q}_{\gamma,m}^{(2)} \quad , \quad (7)$$

where $e_{\gamma}^{(2)}$ is the effective charge of the contribution to the quadrupole operator, coming from the cluster $\gamma = C_1, C_2$ and from the relative motion $\gamma = R$. A geometric estimate of the effective charges is given

in [15], thus, the only parameter in the transition rates in an overall factor, labeled q_{eff} .

To resume: There are three parameters (χ_{n_π} , t_1 , t_3) which are responsible for the position of the band heads, one parameter (χ_{n_π}), which determines the Δn_π dependence of the quadrupole-quadrupole interaction, two parameters which modify the moment of inertia and t_2 , which is responsible for the K -splitting. These parameters are adjusted *in average* to 13-18 energy values, depending on the nucleus, from experiment. The $B(E2)$ transition operator adds the overall scale parameter q_{eff} . This scale factor is adjusted *in average* to 2 $B(E2)$ -values of the ground state band.

In [20] a simple but effective algebraic expression for the spectroscopic factor for a *two cluster system* was proposed. The spectroscopic factor is defined as

$$\begin{aligned}
S = & e^{\mathcal{A}+Bn_\pi+CC_2(\lambda_1,\mu_1)+DC_2(\lambda_2,\mu_2)+EC_2(\lambda_c,\mu_c)} \\
& \times e^{FC_2(\lambda,\mu)+GC_3(\lambda,\mu)+H\Delta n_\pi} \\
& | \langle (\lambda_1, \mu_1) \kappa_1 L_1, (\lambda_2, \mu_2) \kappa_2 L_2 || (\lambda_C, \mu_C) \kappa_C L_C \rangle_{\varrho_C} \\
& \cdot \langle (\lambda_C, \mu_C) \kappa_C L_C, (n_\pi, 0) 1l || (\lambda, \mu) \kappa L \rangle_1 |^2 \quad , \quad (8)
\end{aligned}$$

where the ϱ_C -numbers refer to a multiplicity in the coupling to $SU(3)$ irreps and the κ 's to the multiplicities of the reduction of $SU(3)$ to $SO(3)$. The parameters were adjusted to theoretically exactly calculated spectroscopic factors within the p- and sd-shell, using the $SU(3)$ shell model [21], with excellent results. For the good agreement, the factor depending on the $SU(3)$ -isoscalar factors turns out to be crucial. The parameters \mathcal{A} to H , appearing in (8) are listed in Table 6.

Because the expression in (8) is only valid for a two-cluster system, the results will correspond for ^{20}Ne to $^{16}\text{O}+\alpha$, for ^{24}Mg to $^{20}\text{Ne}+\alpha$ and for ^{28}Si to $^{24}\text{Mg}+\alpha$.

In order to compare some data available in ^{20}Ne , an alternative definition of the spectroscopic factor is used, namely the *dimensional reduced α -width* θ_α^2 [23]

$$\theta_\alpha^2 = \frac{\gamma_\alpha^2}{\gamma_W^2} , \quad (9)$$

where γ_α^2 is the reduced width and γ_W^2 is the *Wigner limit*

$$\gamma_W^2 = \frac{3\hbar^2}{2\mu a^2} , \quad (10)$$

with μ as the reduced mass of the two cluster system and a the channel radius within the R-matrix formulation.

3.2 ^{12}C and ^{16}O summary

In [13, 14] the ^{12}C nucleus, as a three α -particle state, and ^{16}O , as a four α -particle state, were investigated within the SACM, with the motivation to study the role of the *Pauli Exclusion Principle* (PEP). The space for ^{12}C was copied from [12] and the space for ^{16}O was copied from [4]. These spaces agree with the ones constructed with the method proposed in this contribution, except for the multiplicity of one state at $2\hbar\omega$, in the 4α particle system and also in higher shells.

The main point is that the PEP is very important in these systems, leading otherwise to a wrong structure of states at low energy and erroneous interpretations, even when the main degrees of freedom are taken correctly into account. This shows that having identified the correct number of degrees of freedom is not sufficient and that the correct Hilbert space is as important, if not even more.

Observing the PEP, using the SACM leads to a satisfying interpretation of the spectrum so far measured. The SACM shows that other models which take not into account the PEP will lead to a too dense spectrum at low energy. Future experimental studies surely will confirm this, simply because the PEP is a real and important principle of nature.

The ^{12}C and ^{16}O nuclei were investigated in relation to the structure of Hoyle states [5], as the possible formation of α -gas like states [24]. The main theory is described in [25], which uses ab initio methods. In [26] the spatial manifestation of α condensation was investigated, related to a phase transition to an α -gas condensate. Here, we have to emphasize that the SACM is not suited well for the description of an α gas, also due to the present simplified structure of the Hamiltonian.

3.3 ^{20}Ne

One of the rare applications of cluster models to ^{20}Ne is published in [27], where an experimental candidate of a 5- α particle was reported and the interpretation relies on [25]. These multi- α -particle states were related to high-lying 0^+ states. Interesting enough is that the position and sequence of the 0^+ states show a similar behavior in our calculations as in [25]: While the 0^+ states in [25] follow the sequence $E(0_2^+) = 6.06\text{MeV}$, $E(0_3^+) = 11.26\text{MeV}$, $E(0_4^+) = 12.05\text{MeV}$, $E(0_5^+) = 14.03\text{MeV}$, $E(0_6^+) = 14.03\text{MeV}$, in our compilation the sequence is $E(0_2^+) = 6.69\text{MeV}$, $E(0_3^+) = 8.61\text{MeV}$, $E(0_4^+) = 11.95\text{MeV}$, $E(0_5^+) = 12.01\text{MeV}$, $E(0_6^+) = 12.92\text{MeV}$, i.e., the same states of 0_5^+ and 0_6^+ are almost degenerate.

Unfortunately, the model presented here, is too simple for giving realistic contributions to the structure of α gas. However, the multi- α -particle states constructed in Section 2, serve as a practical basis when an ab initio model is used. In [28] some reduced α widths were obtained. Within the SACM these values cannot be compared directly, due to the missing scale factor or the nearly $SU(3)$ symmetry results in zero value. For example, the reduced α width for the 0_2^+ state is 0.17 ± 0.08 , while we obtain $0.10e^{\mathcal{A}}$, where $e^{\mathcal{A}}$ is the scaling factor. From there, adjusting to the deduced value we obtain $e^{\mathcal{A}} = 1.7$. For the 2_2^+ and 4_2^+ state the experimentally deduced values are 0.047 and 0.17, respectively, while we obtain the same value as for 0_1^+ , resulting in the prediction of 0.17, quite well reproducing the experimental observation.

The model Hamiltonian presented above is used to fit the spectrum. Doing so, we have to take into account that ^{20}Ne is a special nucleus, because only those states are considered which are reached in the $^{16}\text{O}(\alpha, \gamma)$ reaction channel. Especially some low-lying negative parity states are not observed in the above mentioned reaction, which makes it difficult to associate the remaining states into bands and compare to the theory.

In Fig. 1 the adjusted spectrum of ^{20}Ne is depicted. On the left hand side, the spectrum is depicted, as obtained with a small $SO(4)$ mixing (i.e., it is essentially $SU(3)$). The position of the band heads is well reproduced. Considering the complex structure of the spectrum and the simple model Hamiltonian, the agreement is satisfactory. In Table 8 some $B(E2)$ -values are listed.

Finally, in Table 9 some spectroscopic factors of $^{16}\text{O} + \alpha \rightarrow ^{20}\text{Ne}$

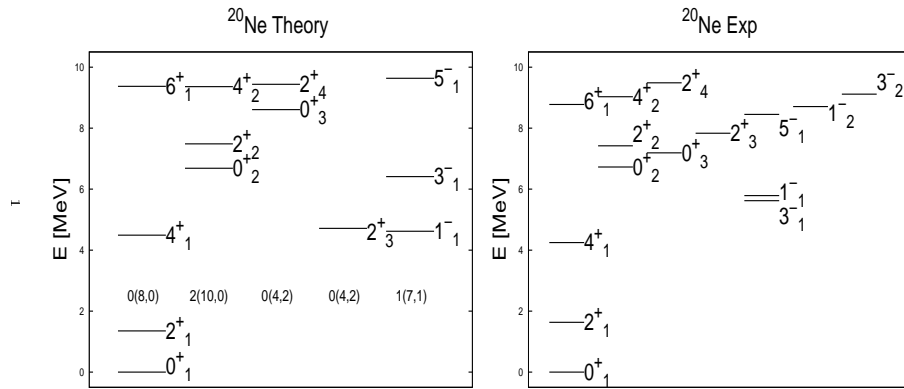


Figure 1: Spectrum of ^{20}Ne , as a 5- α -particle states. The theoretical spectrum (left panel) is compared to experiment (right panel). The theoretical spectrum was obtained including $SO(4)$ mixing. The dominant $\Delta n_\pi(\lambda, \mu)$ quantum numbers are indicated below each band, where Δn_π refers to the number of shell excitations. Experimental data are retrieved from [22].

are tabulated. Also here we see, that ^{20}Ne is special, because several spectroscopic factors different from zero are found. We did also the calculation in the $SU(3)$ -limit, where the parameter b_1 mixing with $SO(4)$ is set to zero. The values of the spectroscopic factors different from zero did not change, nor other non-zero values appeared. The main reason is that the cluster irrep is $(0, 0)$ (the ^{16}O cluster and the α cluster carry both the scalar irrep) the relative irrep is $(8, 0)$, such that for $0\hbar\omega$ only the $(8, 0)$ irrep can be reached and for $2\hbar\omega$ only the $(10, 0)$ irrep can be reached. Due to this characteristic some irreps cannot be reached, as for example the $(4, 2)$ irrep at $0\hbar\omega$ has according to Eq. 8 a zero spectroscopic factor.

3.4 ^{24}Mg

This nucleus is not often considered in the literature, except for example in [24], where even the concept of a n α -particle state was discussed, for up to $n = 10$. Experimental evidence of a 7- α -particle, related to excited states in ^{56}Fe , was reported in [29]. In [30] the cluster α -structure of ^{24}Mg (besides the one of ^{12}C) is investigated using a microscopic cluster approach, with a satisfying agreement. However, instead of a 6- α -particle system the $^{18}\text{O}+\alpha+\alpha$ was considered. In this model, the Hoyle equivalent states show a significant larger root-mean-square radius. In ^{24}Mg two 0^+ states are identified just under the three-body threshold, corresponding to Hoyle equivalent states.

Also for ^{24}Mg the model Hamiltonian of the SACM is too simple to describe these states, but the microscopic model space constructed in this contribution serves as a basis for the description of these states within a full microscopic model.

For the ^{24}Mg nucleus all reaction channels are taken into account and the experimental energies are retrieved from [22]. In Fig. 2 the adjusted spectrum, compared to the experiment, is depicted. On the left hand side, the spectrum, as obtained with $SO(4)$ mixing, is depicted. In Table 8 the $B(E2)$ values are listed and also here the agreement to experiment is quite well.

Finally, In Table 9 predictions for some spectroscopic factors of $^{20}\text{Ne}+\alpha \rightarrow ^{24}\text{Mg}$ are tabulated.

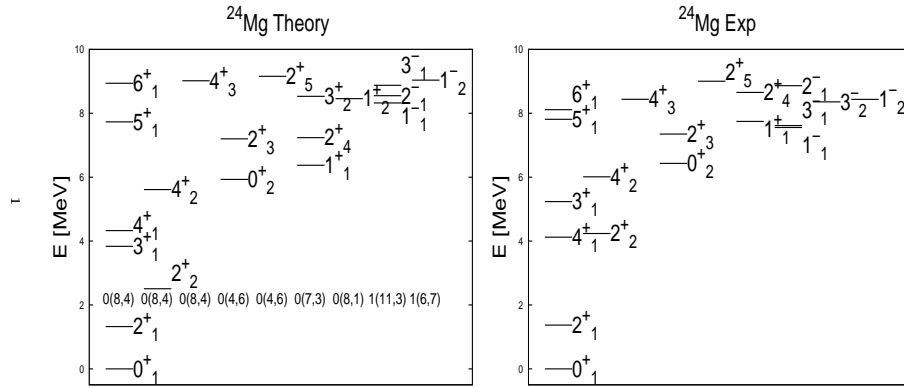


Figure 2: Spectrum of ^{24}Mg , as a 6- α -particle states. The theoretical spectrum (left panel) is compared to experiment (right panel). The theoretical spectrum was obtained, including $SO(4)$ mixing. The dominant $\Delta n_\pi(\lambda, \mu)$ quantum number are indicated below each band, where Δn_π refers to the number of shell excitations. The dominant $\Delta n_\pi(\lambda, \mu)$ quantum numbers are indicated below each band, where Δn_π refers to the number of shell excitations. Experimental data are retrieved from [22].

3.5 ^{28}Si

For ^{28}Si we did not find a relevant detailed discussion, except to the mention of a multi- α particle state in [24]. Nevertheless, the results presented here and the microscopic model space constructed, may be of interest.

This nucleus is in the middle of sd -shell and is already at the limit of validity of the $SU(3)$ model, due to the increase of the spin-orbit interaction. Nevertheless, it may still serve as a good example of a multi- α particle system and simultaneously an approximate $SU(3)$ symmetry.

In Fig. 3.5 the calculated spectrum is shown, with a small $SO(4)$ mixing, on the right hand side, compared to the experimental spectrum on the left hand side. The parameters, used in the $SO(4)$ -mixing, are listed in Table 7. Some calculated $B(E2)$ -values, compared to experiment, are listed in Table 8 and the spectroscopic factors in the $SU(3)$ approximation are listed in Table 9. Note that the spectroscopic factors have decreased even more with respect to the other systems. In general, the heavier the nucleus becomes, the stronger the value of the spectroscopic factor decreases, Though, the ^{28}Si nucleus is a limiting case, the SACM still can describe it fairly well.

4 Conclusions

The main emphasis of this contribution is on the approximate method proposed for the construction of the shell model space for an arbitrary multi- α -particle system. Though, the resulting states are allowed by the *Pauli Exclusion principle*, not all are symmetric under interchange of the α -particles, which is due to the approximation applied. The method is practical and easy to perform for any number of the α -particles. This is one reason to accept the errors, which appear at higher shell excitations and also are related to $SU(3)$ irreps with smaller eigenvalues of the second order Casimir operator, i.e., higher lying states. Apart from the 3-, 4- and 5- α -particle spaces, as a new result we obtained the Hilbert space of 6- and 7- α particles. The agreement to formerly calculated spaces are good, with a disagreement to [4] for the 5- α particle case and $1\hbar\omega$ excitation. However, we could prove that that the low lying states, listed in [4], do not appear in the shell model space.

We hope that the procedure exposed is of great help not only

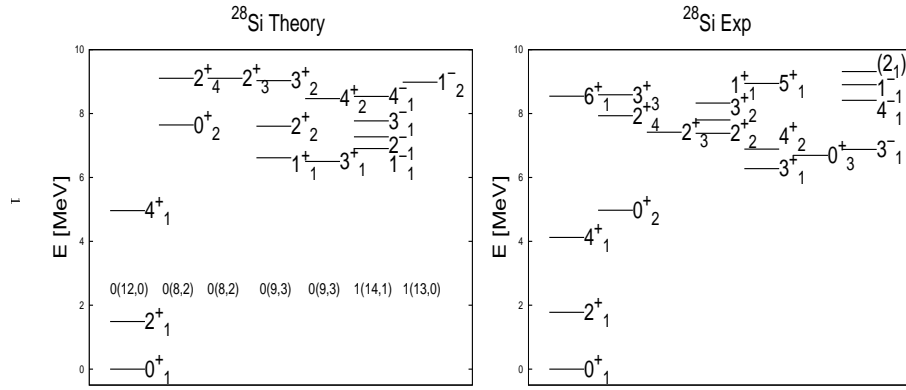


Figure 3: Spectrum of ^{28}Si , as a 7- α -particle states. The theoretical spectrum (left panel) is compared to experiment (right panel). On the left hand side the theoretical spectra, obtained including $SO(4)$ mixing, is depicted, compared to experiment (right hand side). The dominant $\Delta n_\pi(\lambda, \mu)$ quantum numbers are indicated below each band, where Δn_π refers to the number of shell excitations. Experimental data are retrieved from [22].

for an algebraic model, but microscopic theories as well, where the construction of the model space, using numerical procedures, are more involved and/or prohibitive.

The model space was applied within the *Semimicroscopic Algebraic Cluster Model* (SACM) to ^{20}Ne , ^{24}Mg and ^{28}Si , after a short resumé for ^{12}C and ^{16}O was presented. The obtained theoretical spectra and transition values were in fair agreement to experiment. The predicted spectroscopic factors for the $X + \alpha$ system, with X being a multi-cluster α state, show a steady decline with increasing number of α particles. These results may also serve as comparison for more detailed and involved models of a multi- α -particle system [5].

Appendix: Construction of the $1\hbar\omega$ shell model space for the $5-\alpha$ cluster system

In constructing the $5 - \alpha$ -particle system, for the $SU(3)$ content of Pauli allowed states a discrepancy was found to [4] for the $1\hbar\omega$ excitation. The states of the $1\hbar\omega$ excitation $(10, 4)$, $(8, 5)$, $(9, 3)$, $(7, 4)$ and $(5, 5)$, appearing in the Table II of [4], *do not appear in the shell model space we constructed*.

Therefore, in what follows we construct the complete shell model space of ^{20}Ne for $1\hbar\omega$. Because Katō [4] claims that the states constructed are Pauli allowed, they should appear in this shell model space.

First, the general procedure will be explained and afterward the shell model space for $U_{ST}(4)$ irreps mostly antisymmetric is constructed. Non-mostly antisymmetric states belong to higher lying supermultiplets. Nevertheless, at the end all remaining irreps are constructed, i.e., the complete shell model space. We will show that the above mentioned irreps are not contained in the complete $1\hbar\omega$ shell model space and, thus, cannot be anti-symmetric.

General consideration

The classification within each shell η is given by

$$\begin{array}{ccc}
U((\eta + 1)(\eta + 2)) & \supset U(\frac{1}{2}(\eta + 1)(\eta + 2)) \otimes & U_{ST}(4) \\
[1^N] & \begin{array}{c} [\tilde{h}] \\ \cup \\ SU(3) \varrho(\lambda, \mu) \end{array} & [h]
\end{array} \quad , \quad (11)$$

where N is the number of particles in this shell, $[h] = [h_1 h_2 h_3 h_4]$ is the irrep of the spin-isospin group $U_{ST}(4)$ and $[\tilde{h}]$ is the conjugate (interchanging rows with columns) of $[h]$. The $U(\frac{1}{2}(\eta + 1)(\eta + 2))$ group is reduced to $SU(3)$, with (λ, μ) referring to the $SU(3)$ irrep with ϱ its multiplicity. The routines developed in [31] are used.

One usually restricts to $U_{ST}(4)$ irreps of the form $[hhhh]$, $[(h + 1)hhh]$, $[(h + 1)(h + 1)hh]$ or $[(h + 1)(h + 1)(h + 1)h]$, which are due to the supermultiplet structure in nuclei. We can, though, consider also all other possibilities, which will be done later, at the second part of this Appendix.

Procedure:

- Distribute the nucleons in the shell, starting with $0\hbar\omega$.
- En each shell η , fix the $U_{ST}(4)$ irrep, which determines the $U(\frac{1}{2}(\eta + 1)(\eta + 2))$ irrep and reduce to $SU(3)$.
- For a given $n\hbar\omega$ excitation, multiply the results of all shells.
- Suppose we got in this manner the content of the $n\hbar\omega$ excitation. Reduce the center of mass by multiplying the result for $0\hbar\omega$ by $(n, 0)$, the result of $1\hbar\omega$ with $(n - 1, 0)$, etc., until reaching $(n - 1)\hbar\omega$, whose result has to be multiplied by $(1, 0)$. The such obtained list of irreps all correspond to states containing contributions of the center of mass motion and have to be subtracted from the list of multiplying all $SU(3)$ irreps from different shells.
- **The so obtained list of $SU(3)$ irreps correspond to the shell model space of $n\hbar\omega$. The complete space is obtained by using all other possible $U_{ST}(4)$ irreps and repeating the procedure above.**
- The list of Katō [4] should have an overlap to the calculated shell model space. No irrep is allowed to only appear in the list provided by Katō but not in the shell model space!

A: Shell model space for the most antisymmetric irrep of $U_{ST}(4)$

In this section the shell model space, using only the most antisymmetric irrep of $U_{ST}(4)$ is constructed. These $U_{ST}(4)$ irreps are the lowest lying states in energy. In a subsequent section, all the remaining irreps are added, for completeness.

$0\hbar\omega$ space

Here, $\eta = \eta_v$, for η_v the valence shell. The s-shell can be neglected because it is full and contributes only with a $(0, 0)$ irrep.

In case of ^{20}Ne , the 5- α -particle system, there are 4 nucleons in the $\eta = 2$ (sd) shell. The $U_{ST}(4)$ irrep in the sd-shell is $[1^4]$ and thus $[4]$ for $U(6)$. The $SU(3)$ content of this irreps is (we use here and for all reductions the $SU(3)$ library, published in [31]):

$$(8, 0) + (4, 2) + (0, 4) + (2, 0) \quad . \quad (12)$$

This agrees with the table listed in Katō's publication in 1988 [4].

$1\hbar\omega$ space

There are two cases of distributing the nucleons in the shells:

- a) 4 nucleons in the s-shell, 12 in the p-shell, 3 in the sd shell and 1 in the pf-shell. The s- and p-shell do not contribute, because they are closed.
- b) 4 nucleons in the s-shell, 11 (one hole) in the p-shell and 5 nucleons in the sd-shell.

These are all possibilities for the $1\hbar\omega$ excitation.

Case a)

The $SU(3)$ content of 3 particles in the sd shell and of one in the pf-shell, respectively, is (the irrep of $U_{ST}(4)$ is given by $[1^3]_{U_{ST}(4)}$, which corresponds to $[3]$ in $U(6)$),

$$\begin{aligned}
\text{sd} : & \quad (6, 0) + (2, 2) + (0, 0) \\
\text{pf} : & \quad (3, 0) \quad .
\end{aligned} \tag{13}$$

Multiplying the result of the sd-shell with the pf-shell, we obtain:

$$\begin{aligned}
(6, 0) \otimes (3, 0) &= (9, 0) + (7, 1) + (5, 2) + (3, 3) \\
(2, 2) \otimes (3, 0) &= (5, 2) + (3, 3) + (1, 4) + (4, 1) \\
&\quad + (2, 2) + (0, 3) + (3, 0) + (1, 1) \\
(0, 0) \otimes (3, 0) &= (3, 0)
\end{aligned} \tag{14}$$

Case b)

The $SU(3)$ content of 5 particles in the sd shell (we have the $U_{ST}(4)$ irrep $[2, 1^3]$ and therefore in $\eta = 2$ the orbital irrep $[4, 1]_{U(6)}$) and of one hole in the p-shell, respectively, is

$$\begin{aligned}
\text{sd} : & \quad (8, 1) + (6, 2) + (4, 3) + (5, 1) + (2, 4) + (3, 2) + (4, 0) \\
&\quad + (1, 3) + (2, 1) + (0, 2) \\
\text{p} : & \quad (0, 1) \quad .
\end{aligned} \tag{15}$$

Multiplying the result of the sd-shell with the p-shell, we obtain:

$$\begin{aligned}
(8, 1) \otimes (0, 1) &= (8, 2) + (9, 0) + (7, 1) \\
(6, 2) \otimes (0, 1) &= (6, 3) + (7, 1) + (5, 2) \\
(4, 3) \otimes (0, 1) &= (4, 4) + (5, 2) + (3, 3) \\
(5, 1) \otimes (0, 1) &= (5, 2) + (6, 0) + (4, 1) \\
(2, 4) \otimes (0, 1) &= (2, 5) + (3, 3) + (1, 4) \\
(3, 2) \otimes (0, 1) &= (3, 3) + (4, 1) + (2, 2) \\
(4, 0) \otimes (0, 1) &= (4, 1) + (3, 0) \\
(1, 3) \otimes (0, 1) &= (1, 4) + (2, 2) + (0, 3) \\
(2, 1) \otimes (0, 1) &= (2, 2) + (3, 0) + (1, 1) \\
(0, 2) \otimes (0, 1) &= (0, 3) + (1, 1) \quad .
\end{aligned} \tag{16}$$

Intermediate result for the $1\hbar\omega$ excitation

Summing the result for case a) and b), we obtain

$$\begin{aligned}
& (9,0)^2 + (7,1)^3 + (3,3)^5 + (1,4)^3 + (4,1)^4 \\
& + (2,2)^4 + (0,3)^3 + (3,0)^4 + (1,1)^3 + (8,2) + (6,3) \\
& + (5,2)^5 + (4,4) + (6,0) + (2,5) \quad , \quad (17)
\end{aligned}$$

where an upper index denotes the multiplicity.

Removing the center of mass

For this, we multiply all irreps in the $0\hbar\omega$ space, given in (12), by $(1,0)$:

$$\begin{aligned}
(8,0) \otimes (1,0) &= (9,0) + (7,1) \\
(4,2) \otimes (1,0) &= (5,2) + (3,3) + (4,1) \\
(0,4) \otimes (1,0) &= (1,4) + (0,3) \\
(2,0) \otimes (1,0) &= (3,0) + (1,1) \quad . \quad (18)
\end{aligned}$$

All the irreps on the right hand side represent irreps with center of mass contributions and have to be subtracted from the list in (17).

Final result for the $1\hbar\omega$ excitation

Subtracting (18) from (17) leads to the final list

$$\begin{aligned}
& (9,0) + (7,1)^2 + (3,3)^4 + (1,4)^2 + (4,1)^3 \\
& + (2,2)^4 + (0,3)^2 + (3,0)^3 + (1,1)^2 + (8,2) + (6,3) \\
& + (5,2)^4 + (4,4) + (6,0) + (2,5) \quad . \quad (19)
\end{aligned}$$

This list has to be compared with the one of Katō's table [4] for 5 α particles. The list *does not contain the irreps*

$$(10,4) , (8,5) , (9,3) , (7,4) , (5,5) \quad . \quad (20)$$

Thus, for example $(10,4)$ does not have an overlap with the shell model space and cannot satisfy the Pauli exclusion principle. All others are

also not contained, restricting to the *most anti-symmetric irrep of $U_{ST}(4)$ in each shell*. If they are contained using other $U(4)$ irreps will be investigated in the next section. But minimally $(10, 4)$ is *not contained*, because the other $U_{ST}(4)$ irreps will produce $SU(3)$ irreps which are not as large as $(10, 4)$.

B: Completing the shell model space

In this section we will include further irreps of $U_{ST}(4)$, which correspond to supermultiplets at higher energy.

$0\hbar\omega$ excitation

The four missing $U_{ST}(4)$ irreps are $[2, 1^2]_{U_{ST}(4)}$, $[3, 1]_{U_{ST}(4)}$, $[2^2]_{U_{ST}(4)}$ and $[4]_{U_{ST}(4)}$, which imply a $U(6)$ representation (sd-shell) of $[3, 1]_{U(6)}$, $[2, 1^2]_{U(6)}$, $[2^2]_{U(6)}$ and $[1^4]_{U(6)}$, respectively.

The reduction of the $U(6)$ irreps to $SU(3)$ is

$$\begin{aligned}
[3, 1]_{U(6)} &\rightarrow (6, 1) + (4, 2) + (2, 3) + (3, 1) + (1, 2) \\
&\quad + (2, 0) \\
[2, 1^2]_{U(6)} &\rightarrow (5, 0) + (2, 3) + (3, 1) + (1, 2) + (0, 1) \\
[2^2]_{U(6)} &\rightarrow (4, 2) + (3, 1) + (0, 4) + (2, 0) \\
[1^4]_{U(6)} &\rightarrow (1, 2) \quad . \quad (21)
\end{aligned}$$

$1\hbar\omega$ excitation

We use the same notation for case a) and case b).

Case a)

The $[3]_{U(6)}$ was already considered in the former section. The remaining irreps of $U(6)$ are $[2, 1]_{U(6)}$ and $[1^3]_{U(6)}$

The reduction of the $U(6)$ irrep is:

$$\begin{aligned}
\text{sd : } [2, 1] &\rightarrow (4, 1) + (2, 2) + (1, 1) \\
[2, 1] &\rightarrow (3, 0) + (0, 3) \quad . \quad (22)
\end{aligned}$$

This has to be coupled to $(3, 0)$ of the pf-shell:

$$\begin{aligned}
(4, 1) \otimes (3, 0) &= (7, 1) + (5, 2) + (6, 0) + (3, 3) \\
&\quad + (1, 4) + (4, 1) + (2, 2) \\
(2, 2) \otimes (3, 0) &= (5, 2) + (3, 3) + (1, 4) + (4, 1) \\
&\quad + (2, 2) + (0, 3) + (3, 0) + (1, 1) \\
(1, 1) \otimes (3, 0) &= (4, 1) + (2, 2) + (3, 0) + (1, 1) \\
(3, 0) \otimes (3, 0) &= (0, 3) + (2, 2) + (4, 1) + (6, 0) \\
(0, 3) \otimes (3, 0) &= (0, 0) + (1, 1) + (2, 2) + (3, 3) \quad . \quad (23)
\end{aligned}$$

Case b)

The p- $SU(3)$ irrep is the same. The additional sd- $U(6)$ irreps are now $[3, 2]$, $[3, 1^2]$, $[2^2, 1]$, $[2, 1^3]$ and $[1^5]$. The reduction to $SU(3)$ yields

$$\begin{aligned}
[3, 2] &\rightarrow (6, 2) + (4, 3) + (5, 1) + (2, 4) + (3, 2) \\
&\quad + (4, 0) + (1, 3) + (2, 1) + (0, 2) \\
[3, 1^2] &\rightarrow (7, 0) + (4, 3) + (5, 1) + (3, 2) \\
&\quad + (0, 5) + (1, 3) + (2, 1) + (1, 0) \\
[2^2, 1] &\rightarrow (5, 1) + (2, 4) + (3, 2) + (4, 0) + (1, 3) \\
&\quad + (2, 1) + (0, 2) \\
[2, 1^3] &\rightarrow (3, 2) + (1, 3) + (2, 1) + (1, 0) \\
[1^5] &\rightarrow (0, 2) \quad . \quad (24)
\end{aligned}$$

These irreps have to be multiplied by the $(0, 1)$ from the p-shell:

$$\begin{aligned}
(6,2) \otimes (0,1) &\rightarrow (6,3) + (7,1) + (5,2) \\
\text{twice } (4,3) \otimes (0,1) &\rightarrow 2\{(4,4) + (5,2) + (3,3)\} \\
\text{three times } (5,1) \otimes (0,1) &\rightarrow 3\{(5,2) + (6,0) + (4,1)\} \\
\text{twice } (2,4) \otimes (0,1) &\rightarrow 2\{(2,5) + (3,3) + (1,4)\} \\
\text{four times } (3,2) \otimes (0,1) &\rightarrow 4\{(3,3) + (4,1) + (2,2)\} \\
\text{twice } (4,0) \otimes (0,1) &\rightarrow 2\{(4,1) + (3,0)\} \\
\text{four times } (1,3) \otimes (0,1) &\rightarrow 4\{(1,4) + (2,2) + (0,3)\} \\
\text{four times } (2,1) \otimes (0,1) &\rightarrow 4\{(2,2) + (3,0) + (1,1)\} \\
\text{three times } (0,2) \otimes (0,1) &\rightarrow 3\{(0,3) + (1,1)\} \\
(7,0) \otimes (0,1) &\rightarrow (7,1) + (6,0) \\
(0,5) \otimes (0,1) &\rightarrow (0,6) + (1,4) \\
\text{twice } (1,0) \otimes (0,1) &\rightarrow 2\{(1,1) + (0,0)\} \quad . \quad (25)
\end{aligned}$$

Total additional space

Joining the list of irreps of (23) and (25), which correspond to higher lying states of supermultiplets, we arrive at

$$\begin{aligned}
&(4,1)^{13} + (6,0)^6 + (5,2)^8 \\
&+ (3,0)^8 + (3,3)^{11} + (2,2)^{17} + (1,1)^{12} \\
&+(0,0)^3 + (6,3) + (7,1)^3 + (4,4)^2 + (2,5)^2 \\
&+ (1,4)^9 + (0,3)^9 + (0,6) \quad (26)
\end{aligned}$$

Removing the center of mass motion

The additional $SU(3)$ irreps, which contain contributions to the center of mass motion, are obtained multiplying the list in (21) by $(1,0)$:

$$\begin{aligned}
(6,1) \otimes (1,0) &\rightarrow (7,1) + (5,2) + (6,0) \\
(5,0) \otimes (1,0) &\rightarrow (6,0) + (4,1) \\
\text{twice } (4,2) \otimes (1,0) &\rightarrow 2 \{(5,2) + (3,3) + (4,1)\} \\
\text{twice } (2,3) \otimes (1,0) &\rightarrow 2 \{(3,3) + (1,4) + (2,2)\} \\
\text{three times } (3,1) \otimes (1,0) &\rightarrow 3 \{(4,1) + (2,2) + (3,0)\} \\
\text{three times } (1,2) \otimes (1,0) &\rightarrow 3 \{(2,2) + (0,3) + (1,1)\} \\
\text{twice } (2,0) \otimes (1,0) &\rightarrow 2 \{(3,0) + (1,1)\} \\
(0,4) \otimes (1,0) &\rightarrow (1,4) + (0,3) \\
(0,1) \otimes (1,0) &\rightarrow (1,1) + (0,0) \quad . \quad (27)
\end{aligned}$$

This leads to the list of irreps, containing center of mass excitations, which have to be removed from the list in (26).

$$\begin{aligned}
(7,1) + (5,2)^3 + (6,0)^2 + (3,3)^4 + (4,1)^6 + (1,4)^3 + (2,2)^8 \\
+ (3,0)^5 + (1,1)^6 + (0,3)^4 + (0,0) \quad . \quad (28)
\end{aligned}$$

Total additional shell model irreps

Subtracting (28) from (26), leads to the additional appearing $SU(3)$ shell model states

$$\begin{aligned}
(4,1)^7 + (6,0)^4 + (5,2)^5 \\
+ (3,0)^3 + (3,3)^7 + (2,2)^9 + (1,1)^6 \\
+ (0,0)^2 + (6,3) + (7,1)^2 + (4,4)^2 + (2,5)^2 \\
+ (1,4)^6 + (0,3)^5 + (0,6) \quad (29)
\end{aligned}$$

Again, there is no (10,4), (8,5), (9,3), (7,4) neither (5,5) (see (20)) appearing in Katō's list [4].

Acknowledgments

We acknowledge financial support form DGAPA-PAPIIT (IN100421)

References

- [1] K. Wildermuth and Y. C. Tang, *A Unified Theory of the Nucleus* (Friedr. Vieweg & Sohn Verlagsgesellschaft mbH, Braunschweig, 1977).
- [2] M. Freer, H. Horiuchi, Y. Kanada-En'yo, D. Lee and U.-G. Meißner, *Rev. Mod. Phys.* **90** (2018), 035004.
- [3] T. Yamada, Y. Funaki, H. Horiuchi, G. Röpke, P. Schuck and A. Tohsaki, *Nuclear Alpha- Particle Condensates*. In: Beck C. (eds) *Clusters in Nuclei*, Vol.2. *Lecture Notes in Physics*, Vol **848** (Springer, Berlin, Heidelberg, 2012).
- [4] K. Katō, K. Fukatsu and H. Tanaka, *Progress of Theoretical Physics* **80** (1988), 663.
- [5] P. Schuck, *AIP Conf. Proc.* 2038 (2018), 020002.
- [6] J. Cseh, *Phys. Lett. B* **281** (1992), 173.
- [7] J. Cseh and G. Lévai, *Ann. Phys. (N.Y.)* **230**, 165 (1994)
- [8] W. Greiner, J. Y. Park and W. Scheid, *Nuclear Molecules*, (World Scientific, Singapore, 1995).
- [9] P. O. Hess and W. Greiner, *Il Nuovo Cimento* **83**, 76 (1984).
- [10] V. C. Aguilera-Navarro, M. Moshinsky and P. Kramer, *Ann. Phys.* **54** (1969), 379.
- [11] M. Moshinsky and Y. Smirnoc. *The Harmonic Oscillator in Modern Physics*, (Harwood Academic Publishers, Australia, 1996).
- [12] Horiuchi H.; *Prog. Theor. Phys.* **1974**, 51, 1266.
- [13] P. O. Hess, *Eur. Phys. J a* **54** (2018), 32.
- [14] P.O. Hess, J.R.M. Berriel-Aguayo and L.J. Chávez-Nuñez, *Eur. Phys. J. A* **55** (2019), 71.
- [15] H. Yépez-Martínez, M. J. Ermamatov, P. R. Fraser and P. O. Hess, *Phys. Rev. C* **86** (2012), 034309.
- [16] J. Blomqvist and A. Molinari, *Nucl. Phys. A* **106**, 545 (1968)
- [17] Castanos, draayer, leschber *ZfP*, TE, contracted model
- [18] O.Castaños, P.O.Hess, P.Rocheford, J.P.Draayer, *Nucl. Phys.* **A524**, 469 (1991)
- [19] J. Escher and J.P. Draayer, *J. Math. Phys.* 39, 5123 (1998)

- [20] P. O. Hess, A. Algora, J. Cseh and J. P. Draayer, Phys. Rev. **C70**, 051303(R) (2004)
- [21] J. P. Draayer, Nucl. Phys. A **237**, 157 (1975) **check reference**
- [22] National Nuclear Data Center, <http://www.nndc.bnl.gov>
- [23] J. Cseh, G. Lévai and K. Katō, Phys. Rev. C **43** (1991), 165.
- [24] P Schuck, J. Phys.: Conf. Ser. **436** (2013), 012065.
- [25] A Tohsaki, H. Horiuchi, P. Schuck and G. Röpke, Rev. Mod. Phys. **89** (2017), 011002.
- [26] T. Fukui, Y. Kanada-En'yo, K. Ogata, T. Suhara and Y. Taniguchi, Nucl. Phys. A **983** (2019), 38.
- [27] S. Adachi, Y. Fujikawa, T. Kawabata, et al., Phys. Lett. B (2021), in press; arXiv:2008.01632
- [28] H. T. Rickards, Phys. Rev. C **29** (1984), 276.
- [29] H Akimune et al., J. Phys.: Conf. Ser. **436** (2013), 012010.
- [30] P. Descouvemont, arXiv:2101.00955[nucl-th], 2021.
- [31] C. Bahri, D. J. Rowe and J. P. Draayer, Comput. Phys. Commun. **159** (2004), 121.

$n\hbar\omega$	Katō	present compilation
0	(2, 0) (0, 4) (4, 2) (8, 0)	(2, 0) (0, 4) (4, 2) (8, 0)
1	(3, 0) (0, 3) (2, 2) (4, 1) (1, 4) (3, 3) ² (5, 2) ² (2, 5) (4, 4) (7, 1) (6, 3) (9, 0) <i>(5, 5)² (8, 2)² (7, 4)³ (9, 3)²</i> <i>(8, 5) (10, 4)</i>	<i>(1, 1)²</i> (3, 0) ³ (0, 3) ² (2, 2) ⁴ (4, 1) ³ (1, 4) ² (3, 3) ⁴ <i>(6, 0)</i> (5, 2) ⁴ (2, 5) (4, 4) (7, 1) ² (6, 3) (9, 0) (8, 2)
2	(0, 2) ² (2, 1) (1, 3) ² (4, 0) ³ (3, 2) ² (2, 4) ⁵ (5, 1) ³ (4, 3) ⁴ (1, 6) ² (3, 5) ² (6, 2) ⁶ (5, 4) ⁵ (0, 8) (8, 1) ⁴ (4, 6) ⁴ (7, 3) ⁶ (6, 5) ⁶ (10, 0) ³ (9, 2) ² (8, 4) ¹⁰ (11, 1) <i>(7, 6)² (10, 3)⁴ (9, 5)⁴</i> <i>(11, 4)² (13, 3)</i>	<i>(1, 0)</i> (0, 2) ⁶ (2, 1) ¹⁰ (1, 3) ¹¹ (4, 0) ¹³ (3, 2) ¹⁴ <i>(0, 5)</i> (2, 4) ¹⁵ (5, 1) ¹² (4, 3) ¹⁴ (1, 6) ² <i>(7, 0)</i> (3, 5) ⁴ (6, 2) ¹⁴ (5, 4) ⁴ (0, 8) (8, 1) ⁵ (4, 6) ² (7, 3) ³ (6, 5) (10, 0) ³ (9, 2) (8, 4) (11, 1)
3	(0, 1) (1, 2) ³ (3, 1) ⁴ (0, 4) (2, 3) ⁶ (5, 0) ⁴ (4, 2) ⁶ (1, 5) ⁵ (3, 4) ⁹ (6, 1) ⁶ (0, 7) ² (5, 3) ¹¹ (2, 6) ⁵ (8, 0) ³ (4, 5) ⁹ (7, 2) ¹¹ (1, 8) ² (6, 4) ⁹ (3, 7) ⁴ (9, 1) ⁴ (5, 6) ⁶ (8, 3) ¹² (2, 9) (7, 5) ¹⁶ (4, 8) (11, 0) ⁴ (10, 2) ⁵ (6, 7) ³ (9, 4) ¹⁸ (8, 6) ¹² (12, 1) (11, 3) ⁸ <i>(10, 5)⁸ (13, 2) (12, 4)⁴ (14, 3)²</i>	(0, 1) ⁶ <i>(2, 0)¹¹</i> (1, 2) ³¹ (3, 1) ⁴⁷ (0, 4) ¹⁹ (2, 3) ⁶⁰ (5, 0) ⁴² (4, 2) ⁶⁸ (1, 5) ⁶⁸ (3, 4) ⁶³ (6, 1) ⁴⁸ (0, 7) ⁸ (5, 3) ⁶² (2, 6) ¹⁵ (8, 0) ¹² (4, 5) ²⁵ (7, 2) ⁴⁵ (1, 8) ³ (6, 4) ²⁰ (3, 7) ⁵ (9, 1) ¹⁹ (5, 6) ⁶ (8, 3) ¹³ (2, 9) (7, 5) ⁴ (4, 8) (11, 0) ⁸ (10, 2) ⁴ (6, 7) (9, 4) ² (8, 6) (12, 1) ² (11, 3)

Table 3: Space of the 5- α -particle system. In bold-face in the left column the different multiplicity is indicated, compared to the right column. In italic we denote the irreps in the right column which do not appear in the left column. (For color online: The blue tainted irreps in the left column refer to those not appearing in the present compilation. The blue irreps in the right column appear only in the present compilation and the red tainted multiplicities are larger than in Katō's compilation). Note, as an example, the (10, 4) irreps on the left side, which is not present on the right side. In the Appendix we prove that this state has to be excluded because it is not part of the shell model space.

$n\hbar\omega$	$6 - \alpha$
0	$(0, 2) (1, 3) (4, 0)^2 (3, 2) (2, 4)^2 (5, 1)^2 (4, 3)$ $(3, 5) (6, 2)^2 (5, 4) (0, 8) (8, 1) (4, 6) (7, 3)$ $(8, 4)$
1	$(0, 1)^3 (2, 0)^5 (1, 2)^{12} (3, 1)^{16} (0, 4)^7 (2, 3)^{21} (5, 0)^{12}$ $(4, 2)^{24} (1, 5)^{13} (3, 4)^{22} (6, 1)^{20} (0, 7)^4 (5, 3)^{22} (2, 6)^{10}$ $(8, 0)^8 (4, 5)^{13} (7, 2)^{16} (1, 8)^3 (6, 4)^{11} (3, 7)^5 (9, 1)^7$ $(5, 6)^6 (8, 3)^7 (2, 9) (7, 5)^4 (11, 0) (10, 2)^3 (6, 7)$ $(9, 4)^2 (11, 3)$
2	$(0, 0)^9 (1, 1)^{32} (3, 0)^{27} (0, 3)^{27} (2, 2)^{93} (4, 1)^{85} (1, 4)^{70}$ $(3, 3)^{119} (6, 0)^{62} (0, 6)^{39} (2, 5)^{80} (5, 2)^{109} (4, 4)^{115} (7, 1)^{78}$ $(1, 7)^{34} (3, 6)^{55} (6, 3)^{92} (5, 5)^{61} (9, 0)^{25} (0, 9)^4 (2, 8)^{28}$ $(8, 2)^{66} (7, 4)^{44} (4, 7)^{23} (10, 1)^{25} (1, 10)^2 (6, 6)^{25} (3, 9)^4$ $(9, 3)^{28} (5, 8)^3 (8, 5)^{14} (12, 0)^7 (0, 12) (11, 2)^{10} (7, 7)^2$ $(4, 10) (10, 4)^9 (9, 6) (13, 1)^2 (12, 3)^3 (11, 5) (14, 2)$

Table 4: Space of the $6-\alpha$ -particle system, with the same observations as in Table 2.

$n\hbar\omega$	$7 - \alpha$
0	$(0, 0)^2 (2, 2)^3 (4, 1)(1, 4)(3, 3)^3(6, 0)^3(0, 6)^3$ $(2, 5) (5, 2) (4, 4)^4 (7, 1) (1, 7) (3, 6)^2 (6, 3)^2$ $(5, 5)^2 (8, 2)^2 (2, 8)^2 (6, 6)/(9, 3) (3, 9) (12, 0)$ $(0, 12)$
1	$(1, 0)^6 (0, 2)^8 (2, 1)^{23} (1, 3)^{29} (4, 0)^{14} (3, 2)^{44} (0, 5)^{20}$ $(2, 4)^{43} (5, 1)^{34} (4, 3)^{53} (1, 6)^{64} (7, 0)^{70} (3, 5)^{46} (6, 2)^{36}$ $(5, 4)^{44} (0, 8)^{10} (2, 7)^{29} (8, 1)^{20} (4, 6)^{29} (7, 3)^{27} (1, 9)^{11}$ $(6, 5)^{22} (3, 8)^{15} (10, 0)^5 (9, 2)^{15} (5, 7)^{10} (8, 4)^{12} (0, 11)^3$ $(2, 10)^5 (7, 6)^6 (11, 1)^5 (4, 9)^4 (10, 3)^6 (6, 8)^2 (9, 5)^2$ $(1, 12) (3, 11) (13, 0) (8, 7) (12, 2)^2 (5, 10) (11, 4) (14, 1)$
2	$(0, 1)^{22} (2, 0)^{68} (1, 2)^{113} (3, 1)^{163} (0, 4)^{110} (2, 3)^{225} (5, 0)^{88}$ $(4, 2)^{282} (1, 5)^{189} (3, 4)^{284} (6, 1)^{185} (0, 7)^{72} (5, 3)^{284} (2, 6)^{229}$ $(8, 0)^{95} (4, 5)^{249} (7, 2)^{184} (1, 8)^{100} (6, 4)^{226} (3, 7)^{159} (9, 1)^{99}$ $(5, 6)^{146} (8, 3)^{138} (0, 10)^{33} (2, 9)^{60} (7, 5)^{115} (4, 8)^{77} (11, 0)^{23}$ $(10, 2)^{79} (6, 7)^{54} (1, 11)^{17} (9, 4)^{64} (3, 10)^{21} (8, 6)^{38} (5, 9)^{20}$ $(12, 1)^{26} (11, 3)^{34} (7, 8)^{11} (2, 12)^5 (10, 5)^{16} (4, 11)^3 (14, 0)^8$ $(9, 7)^7 (6, 10)^4 (13, 2)^{12} (12, 4)^9 (3, 13) (8, 9) (11, 6)^2$ $(15, 1)^5 (14, 3)^2 (10, 8) (13, 5) (17, 0) (16, 2)$

Table 5: Space of the $7-\alpha$ -particle system, with the same observations as in Table 2.

\mathcal{A}	B	C	D
-	-0.36113	-0.054389	-0.11764
E	F	G	H
0.060728	-0.0086654	0.000021097	1.9090

Table 6: Parameter values used for the spectroscopic factor of (8).

Parameter	^{20}Ne	^{24}Mg	^{28}Si
$\hbar\omega$	13.19	12.60	12.11
χ	-0.406628	-0.177055	-0.0737703
ξ	0.124941	0.194327	0.223200
t_1	0.00134669	6.88122×10^{-4}	-3.45015×10^{-3}
t_2	-0.0333108	0.314263	-0.317268
$\chi_{n\pi}$	-0.197490	-0.0942936	-0.0674217
$\xi_{L_{np}}$	-0.0473878	-0.145655	-0.16083
b_1	-0.350871	0.188599	-0.101639
t_3	0.00234264	-6.31156×10^{-5}	3.91536×10^{-4}
q_{eff}	0.2930	0.290611	0.27301

Table 7: Non-zero parameter values for ^{20}Ne , ^{24}Mg and ^{28}Si .

$J_i^{P_i} \rightarrow J_f^{P_f}$	^{20}Ne Th	^{24}Mg th	^{28}Si th	$B(E_2)[\text{Ne}]$	$B(E_2)[\text{Mg}]$	$B(E_2)[\text{Si}]$
$2_1^+ \rightarrow 0_1^+$	21.78	25.97	15.54	20.3 ± 1	21.5 ± 1.0	13.2 ± 0.5
$2_1^+ \rightarrow 0_2^+$	0.38	0.095	0	0.027	0.128 ± 0.02	-
$2_1^+ \rightarrow 0_3^+$	0	0.0013	0	-	-	0.053 ± 0.003
$2_2^+ \rightarrow 0_1^+$	37.79	2.29	0.012	-	1.94 ± 0.19	0.37 ± 0.15
$2_2^+ \rightarrow 0_2^+$	72.09	0.071	5.92	-	1.78 ± 0.28	0.8 ± 0.5
$2_2^+ \rightarrow 0_3^+$	0	7.87×10^{-4}	0	-	-	-
$2_2^+ \rightarrow 2_1^+$	0	8.96	2.6×10^{-5}	0.73 ± 0.09	-	-
$4_1^+ \rightarrow 2_1^+$	20.78	36.13	20.55	22 ± 2	39 ± 4	16.4 ± 1.8
$2_3^+ \rightarrow 0_1^+$	0	0.0035	0.023	0.73	0.67 ± 0.23	0.162 ± 0.018
$2_3^+ \rightarrow 0_2^+$	0	16.90	7.56	-	0.36 ± 0.004	-
$4_1^- \rightarrow 2_1^-$	0	57.73	47.15	1.8	-	-
$4_1^- \rightarrow 3_1^-$	0	27.54	18.41	-	-	0.91 ± 0.19

Table 8: Theoretical $B(E2)$ -transition values of the systems ^{20}Ne , ^{24}Mg and ^{28}Si . The unit is in WU and the theoretical values are compared to available experimental data [22]. When the theoretical values is 10^{-7} or less, the tabulated value is set to zero.

J_k^P	^{20}Ne (th)	^{24}Mg (th)	^{28}Si
0_1^+	0.2248	0.0001928	$1. \times 10^{-6}$
0_2^+	0.1027	0.0002546	2×10^{-6}
2_1^+	0.2241	0.00007083	2×10^{-7}
2_2^+	0.1034	0.00001039	3×10^{-7}
4_1^+	0.2217	2.325×10^{-6}	7×10^{-8}
4_2^+	0.1057	0.00008475	4×10^{-7}
1_1^-	0.1365	0.00001498	8×10^{-8}
3_1^-	0.1365	0.00005610	3×10^{-7}
5_1^-	0.1365	0.00005075	1×10^{-7}

Table 9: Some spectroscopic factors, divided by $e^{\tilde{A}}$, of low lying states. In the first column the state considered is listed. The spectroscopic factors correspond to a two cluster system of the type $X + \alpha$, where X is a also a multi- α -particle state.